doi:10.1016/j.jmb.2010.01.019 J. Mol. Biol. (2010) 397, 290–300

JMB

Available online at www.sciencedirect.com

ScienceDirect

ELSEVIER

Crystal Structure of *Escherichia coli* Enterobactin-specific Isochorismate Synthase (EntC) Bound to its Reaction Product Isochorismate: Implications for the Enzyme Mechanism and Differential Activity of Chorismate-utilizing Enzymes

Sudharsan Sridharan[1], Nigel Howard[2], Olivier Kerbarh[2], Michał Błaszczyk[1], Chris Abell[2]* and Tom L. Blundell[1]

[1]*Department of Biochemistry, University of Cambridge, 80 Tennis Court Road, Cambridge CB2 1GA, UK*

[2]*Department of Chemistry, The University Chemical Laboratory, Lensfield Road, Cambridge CB2 1EW, UK*

Received 20 July 2009; received in revised form 7 January 2010; accepted 7 January 2010
Available online 15 January 2010

EntC, one of two isochorismate synthases in *Escherichia coli*, is specific to the biosynthesis of the siderophore enterobactin. Here, we report the crystal structure of EntC in complex with isochorismate and Mg^{2+}at 2.3 Å resolution, the first structure of a chorismate-utilizing enzyme with a non-aromatic reaction product. EntC exhibits a complex α+β fold like the other chorismate-utilizing enzymes, such as salicylate synthase and anthranilate synthase. Comparison of active site structures allowed the identification of several residues, not discussed previously, that might be important for the isochorismate activity of the EntC. Although EntC, MenF and Irp9 all convert chorismate to isochorismate, only Irp9 subsequently exhibits isochorismate pyruvate lyase activity resulting in the formation of salicylate and pyruvate as the reaction products. With a view to understanding the roles of these amino acid residues in the conversion of chorismate to isochorismate and to obtaining clues about the pyruvate lyase activity of Irp9, several mutants of EntC were generated in which the selected residues in EntC were substituted for those of Irp9: these included A303T, L304A, F327Y, I346L and F359Q mutations. Biochemical analysis of these mutants indicated that the side chain of A303 in EntC may be crucial in the orientation of the carbonyl to allow formation of a hydrogen bond with isochorismate. Some mutations, such as L304A and F359Q, give rise to a loss of catalytic activity, whereas others, such as F327Y and I346L, show that subtle changes in the otherwise closely similar active sites influence activity. We did not find a combination of these residues that conferred pyruvate lyase activity.

Keywords: chorismate-utilizing enzymes; siderophores; enterobactin; EntC; chorismate isochorismate

Edited by M. Guss

Introduction

Iron-chelating siderophores are essential for the survival of pathogenic bacteria under the iron-deficient conditions inside a human host. Enterobactin is the most powerful iron chelator known, with an estimated association constant of 10^{52} M^{-1} and is used by some bacteria to compete effectively for iron from their environment.[1] Chorismate, the product of the shikimate pathway, is successively converted in *Escherichia coli* by the enzymatic activities of EntC,[2,3] EntB[4,5] and EntA[6] to 2,3-dihydroxybenzoate, from which enterobactin is produced by EntE,[5] EntD[5] and EntF.[7] The genes responsible for the biosynthesis of enterobactin are arranged in two bidirectional clusters. The *entCEBA(X)* operon forms one cluster and *entD* and *entF* are encoded in the other. The open reading frame *entX*, which follows *entA* in the same operon is of unknown function.[8,9]

EntC catalyses the conversion of chorismate to isochorismate (Fig. 1). The enzyme belongs to a

*Corresponding author. E-mail address: ca26@cam.ac.uk.
Present address: S. Sridharan, MedImmune, Aaron Klug Building, Granta Park, Cambridge, CB21 6GH, UK.

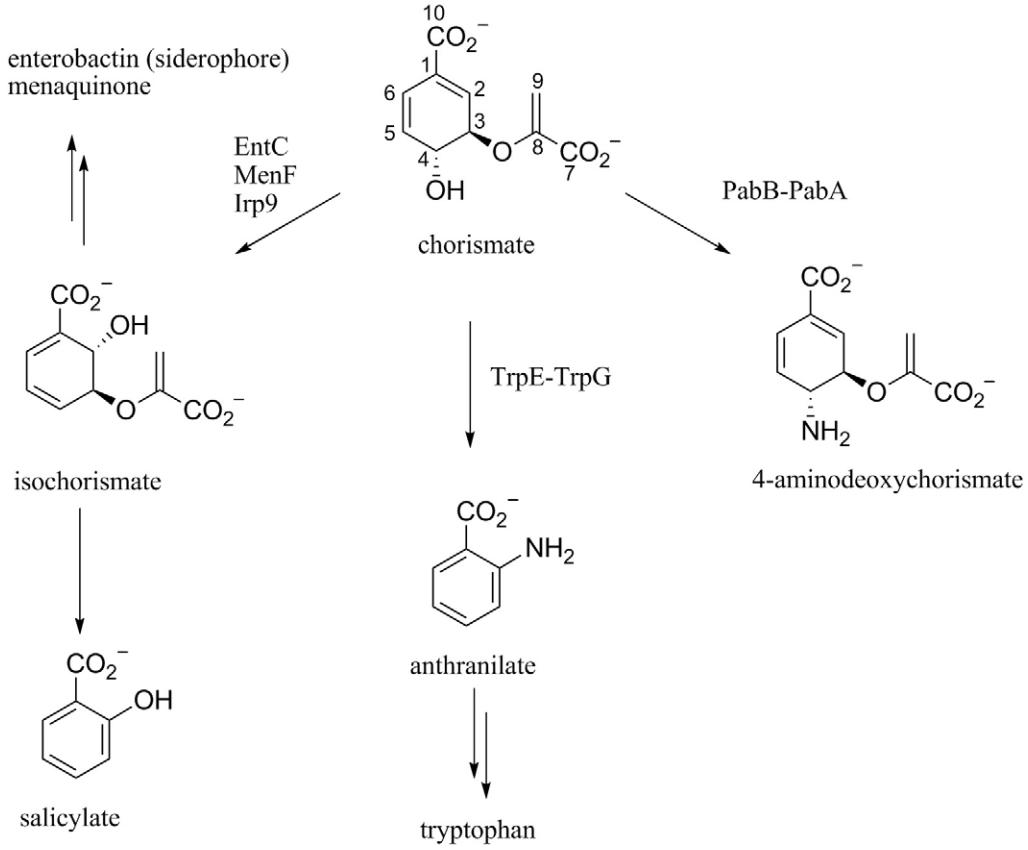

Fig. 1. Transformations catalysed by chorismate-utilizing enzymes.

superfamily that utilize chorismate as the substrate (Fig. 1).[10] The isochorismate synthase activity of EntC is specific to the enterobactin biosynthesis pathway. In addition, *E. coli* has a menaquinone biosynthesis pathway-specific isochorismate synthase activity encoded by the *menF* gene.[11–13] Enterobactin is synthesised under iron-deficient conditions, whereas menaquinones are required for electron transport under anaerobic conditions. As a consequence, the gene clusters responsible for the synthesis of enterobactin and menaquinones are regulated differently. Buss *et al.* also showed that in *E. coli* there is channelling of isochorismate in both these pathways and this may be related to the relative chromosomal positions of the genes responsible for the biosynthesis of these two compounds in their respective gene clusters.[14]

The X-ray crystal structures of several chorismate-utilizing enzymes are known. Knochel *et al.* first reported the structure of *Sulfolobus solfataricus* anthranilate synthase TrpE/TrpG.[15] The structures of anthranilate synthase homologues from *Salmonella typhimurium*[16] and *Serratia marcescens*[17] were subsequently solved. We reported the first structure of a salicylate synthase (*Yersenia enterocolitica* Irp9)[18] and the structure of its homologue from *Mycobacterium tuberculosis* was subsequently described.[19] The structure of *E. coli* isochorismate synthase MenF was reported by Kolappan *et al.*[10] and, more recently, a structure of MenF with $Mg^{2+}$and sulfate bound in the active site was reported.[20] A tryptophan binding site has been identified in anthranilate synthase (TrpE component) and aminodeoxychorismate synthase (PabB) .[21] Tryptophan is involved in feedback inhibition of anthranilate synthase but appears to play only a structural role in PabB.[21]

Chorismate-utilizing enzymes catalyse distinct transformations of chorismate (Fig. 1). The reactions all involve initial loss of the C4 hydroxyl group. In the reaction catalysed by isochorismate synthase this is replaced by a water molecule that attacks at C4; however, the precise mechanism for this reaction is not known.[10] In anthranilate synthase (TrpE-TrpG complex) the nucleophile at C2 is ammonia, which is generated by the glutaminase (TrpG) subunit and transferred to the bifunctional TrpE subunit. [15] The TrpE subsequently performs the conversion of chorismate to 2-aminodeoxychorismate, followed by the elimination of pyruvate (pyruvate lyase activity). Salicylate synthase (Irp9) is a bifunctional enzyme that initially catalyses the conversion of chorismate to isochorismate and the subsequent formation of salicylate and pyruvate.[22,23] In PabB, the side chain of Lys274 acts as the C2 nucleophile to form an enzyme-bound intermediate that subsequently reacts at C4 with ammonia, which is generated by an associated glutaminase (PabA).[24,21]

Here, we report the first X-ray crystal structure of *E. coli* EntC bound to isochorismate. The roles of

some of the residues in and close to the active site have been studied using biochemical assays of specific mutants. The mutated residues were chosen primarily on the basis of structural comparison with Irp9. We have identified residues in order to address the question of why EntC catalyses only the chorismate to isochorismate conversion, whereas Irp9 also catalyses the subsequent conversion of isochorismate to salicylate.

Results and Discussion

Structure of EntC

The structure of *E. coli* EntC (Fig. 2) was solved using single isomorphous replacement with anomalous scattering with wild type and selenomethionyl derivative datasets. The structure was refined at 2.3 Å resolution with a final *R*-factor of 20.0% and an R_{free} of 25.5% (Table 1). There are two protein molecules, each with an isochorismate molecule bound in the active site, 293 water molecules, and four magnesium ions (two per protein molecule) in the asymmetric unit. The two protein molecules in the asymmetric unit are related by improper non-crystallographic symmetry. Clear electron density was observed for residues 14–391 for both protein chains in the asymmetric unit. The C^{α} positions of the two chains could be superposed with an RMSD of 0.35 Å.

EntC adopts an α+β fold similar to that of the known structures of other chorismate-utilizing enzymes.[15] The overall structure has nine α-helices and 18 β-strands. Strands β2, β3, β7 and β11 form a twisted β-sheet, which makes an orthogonal β-sandwich with a second twisted sheet formed from strands β5, β6, β17 and β18. Residues L212, A213, G214 and S215 of β15 together with H276 of β17 line the active site. The α-helices lie on the surface of the molecule.

Superposition of the structures of the *E. coli* menaquinone-specific isochorismate synthase (MenF) and EntC demonstrates the existence of additional secondary structural elements in MenF formed by residues 1–40 and 118–154. Similarly, the structures of other chorismate-utilizing enzymes show additional secondary structural elements in the *N*-terminal halves when compared with the EntC structure. EntC contains a helix, labelled α2a (Figs. 2 and 3; and Supplementary Data Fig.S1; secondary structural elements of EntC labelled following the scheme of ssTrpE[15]), which is not seen in any of the structures compared here. α2a is located between β7 and β9, which are common to all these structures. Its position is almost perpendicular to that of α1, as seen in all other structures compared here, except in EntC. β7 continues as β8, which is absent from EntC. The presence of α2a and its positioning are both unique to EntC amongst the chorismate-utilizing enzymes. EntC has the shortest sequence (391 residues) and the most compact structure of this family and may be regarded as the representative core enzyme. Although EntC has only 20–28 % sequence identity with other family members, they exhibit a high degree of structural similarity (Supplementary Data Table 1). As can be seen in the structure-based sequence alignment for representative proteins (Fig. 3), the most conserved region is towards the *C*-terminus.

The active site of EntC

The active site of EntC is located at the base of a cleft formed by parts of α7, β15, and the loops or turns between α8 and α9, β18 and β19, β19 and β20, and β21 and α10 (Fig. 2a). In the active site there is clear density for isochorismate, the product of the EntC-catalysed reaction, and a magnesium ion (Supplementary Data Fig. S3). The ring of the isochorismate lies approximately between the side chain of a conserved lysine (K380) on one side and the carbonyl of the peptide bond between L212 and A213 on the other (Fig. 2b). The C2 hydroxyl of the isochorismate is hydrogen bonded to the carbonyl of A303. The enol-pyruvyl group of the bound isochorismate is sandwiched between the side chains of K380 and I346. One of the enol-pyruvyl carboxylate oxygens is hydrogen bonded to the η1 and ε-nitrogens of R347 and the other is hydrogen bonded to the backbone amide nitrogen of G361 and a water molecule. This water molecule makes a hydrogen bond with the backbone amide nitrogen of R347 and backbone carbonyl of F359 (Fig. 4a). The magnesium ion is coordinated by the C1 carboxylate of isochorismate and the side chains of conserved E241 and E376 residues (Fig. 4a).

This is the first structure in which a non-aromatic product is found bound at the active site of a chorismate-utilizing enzyme. The positions of the isochorismate ring and enol-pyruvyl side chain bound in the active site of EntC are very similar to those of the salicylate ring and pyruvate, respectively, bound in the active site of salicylate synthase (Irp9) (Fig. 4c). The interactions of the bound products are correspondingly similar. The magnesium ion is bound in identical positions in EntC, MenF, and Irp9, with equivalent ligands (Fig. 4; Supplementary Data Fig. S2). The mutation of the arginine residue (R387A) in MenF that corresponds to R347 in the pyruvyl binding pocket in EntC has been reported to result in inactive enzyme.[10]

There are several residues in EntC thought to be involved in catalysis that are conserved amongst the chorismate-utilizing enzymes (Fig. 4a). K147 corresponds to K190 in MenF, which was proposed to act as the catalytic base by activating a nucleophilic water molecule, which is also seen hydrogen bonded to the C2 hydroxyl of isochorismate in the active site. The carboxyl group of E197 (MenF E240) points towards C4 of the bound isochorismate, and is thought to act as the general acid for the loss of the C4 hydroxyl group from chorismate. This is consistent with the observation that MenF E240Q is inactive (Scheme 1).

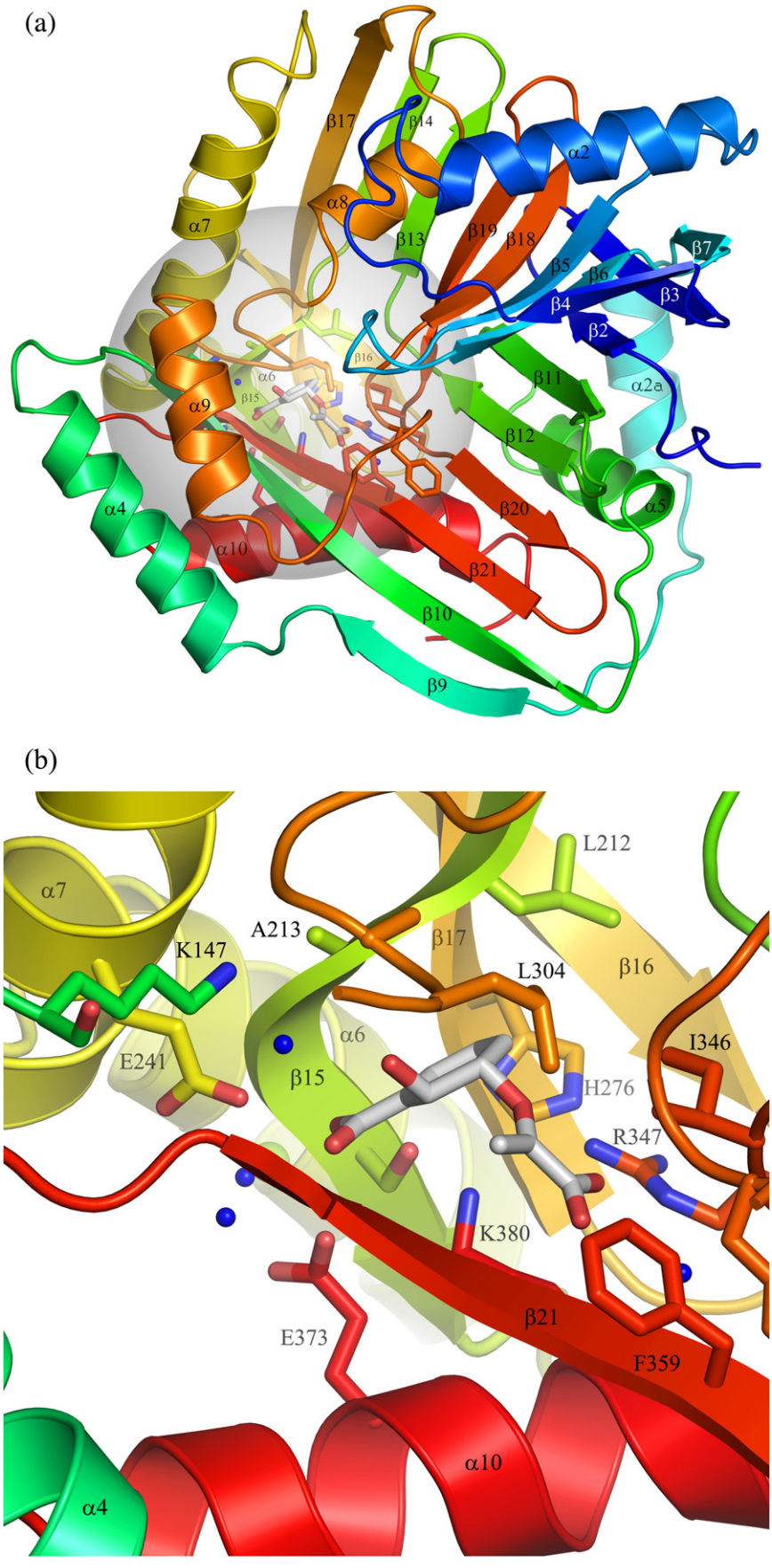

Fig. 2 (*legend on next page*)

Table 1

	Native	Se peak
A. *Data collection*		
Space group	$P2_12_12_1$	$P2_12_12_1$
Resolution (Å)	50.0–2.30	30.0–3.0
No. unique reflections	41,386	18,988
Unit cell dimensions		
a **(Å)**	62.5	62.5
b **(Å)**	104.8	104.5
c **(Å)**	140.0	140.1
$\alpha = \beta = \gamma$ (°)	90.0	90.0
Matthews coefficient (%)	2.58 (52.3)	2.66 (53.8)
High resolution shell (Å)	2.36–2.30	3.11–3.0
$I/\sigma I$ overall	12.4 (1.6)	16.3 (4.6)
Completeness overall	99.9 (99.8)	100 (100)
Redundancy overall	6.4 (5.1)	14.7 (14.9)
Phasing power		
ISO (acentric/centric)	0.36/0.30	—
ANO	0.82	—
FOM (acentric/centric)	0.133/ 0.085	—
B. *Refinement statistics*		
Resolution (Å)	50.0-2.30	—
No. reflections in test set	2088	—
No. reflections in working set	39292	—
No. protein molecules in asymmetric unit	2	—
No. protein atoms in asymmetric unit	5856	—
No. water molecules in asymmetric unit	297	—
R-factor (%)	20.0	—
R_{free} (%)	25.5	—
RMSD from ideal		—
Bond lengths (Å)	0.01	—
Bond angles (°)	1.4	—
Average *B*-factors (Å^2)		—
Main chain	46.0	—
Side chain and water molecules	48.6	—
RMS B main chain	1.9	—
RMS B side chain	3.8	—

Values within parentheses are for the highest resolution shell.

Studies on wild type and mutant forms of EntC

Structural alignment and comparison of the active sites of EntC, MenF and Irp9 reveals a high degree of conservation and points of differences. The residues corresponding to K147, E197, L212-S215, E241, H276, R347, A360-A362, E376 and K380 are conserved among these enzymes (Figs. 3 and 4). H276, L212-S215 and A360-A362 interact directly with the product in EntC. The nearby residues A303, L304 and I346 are not strictly conserved in the three enzymes. A303 is conserved between EntC and MenF but replaced by threonine in Irp9. L304 is substituted by valine in MenF and alanine in Irp9. I346 is replaced by leucine in both MenF and Irp9. Structural comparison also reveals that the residues near the enol-pyruvyl carboxylate of the bound isochorismate are not conserved in these enzymes. There is phenylalanine at positions 327 and 359 in EntC, whereas MenF has tyrosine (Y368 and Y399) and Irp9 has a tyrosine (Y372) and a glutamine (Q403) at equivalent positions. Interestingly, the orientations of the side chains of F327 and F359 in EntC are significantly different from the equivalent residues in MenF and Irp9 (Fig. 4; Supplementary Data Fig. S2). Among the five enzymes compared in the structural alignment (Fig. 3; Supplementary Data Fig. S1) only EntC shows F327 pointing away from the active site with the $C^{\varepsilon 1}$ atom of the ring approximately occupying the position of C^{ζ} atom of MenF Y399. In Irp9, the equivalent tyrosine (Y372) points towards the active site with its side chain hydroxyl oxygen at a distance of 2.5 Å from O1 of the bound pyruvate. The equivalent tyrosine residues in MenF and TrpE and the tryptophan in PabB point towards the active site in these enzymes. The residue at position 359 is not conserved in the five chorismate-utilizing enzymes compared here. F359 of EntC points towards the active site and its ring partially occupies the position of Y372 in Irp9. The equivalent tyrosine (Y399) in MenF points away from the active site in the direction of and partially occupying the position of the EntC F327 ring. The implications of these differences are discussed later.

EntC, MenF and Irp9 all convert chorismate to isochorismate; however, only Irp9 subsequently exhibits isochorismate pyruvate lyase activity resulting in the formation of salicylate and pyruvate as the reaction products. Several active site residues of chorismate-utilizing enzymes have been studied using mutation analysis to understand the roles of these residues in catalysis of these enzymes.[16,21] We have attempted single, double, triple and quadruple amino acid substitutions in EntC (Table 2) at the non-conserved positions 303, 304, 327, 346 and 359, in an attempt to shed light on the roles of these residues in EntC activity and to gain an understanding of the differences in activity compared to Irp9. We chose to substitute the residues at these positions in EntC with the equivalent residues from Irp9 (i.e. A303T, L304A, F327Y, I346L and F359Q) in order to see if any of these substitutions singly or in combination with others could impart salicylate synthase activity to EntC.

The various mutant EntC enzymes containing double, triple and quadruple amino acid substitutions (Table 2) either have significantly reduced isochorismate synthase activity or are inactive. As described in Materials and Methods, salicylate production was monitored in the absence of PchB (which converts isochorismate to salicylate). In these assays, neither wild type EntC nor any of the mutant enzymes showed any salicylate synthase activity.

Residues A303, L304, I346 are aligned over C3 and the enolpyruvate group of isochorismate (Fig. 4a), with the backbone carbonyl oxygen of A303 only

Fig. 2. (a) The structure of *E. coli* EntC shown in cartoon representation using rainbow colours from the N to the C terminus. The bubble encompasses the active site region of EntC, shown enlarged in (b). Isochorismate, grey; magnesium ion, green sphere; and water, blue sphere. Several active site residues are shown but, for clarity, only the side chains of the residues are shown. The figures were generated using PyMOL (www.pymol.org).

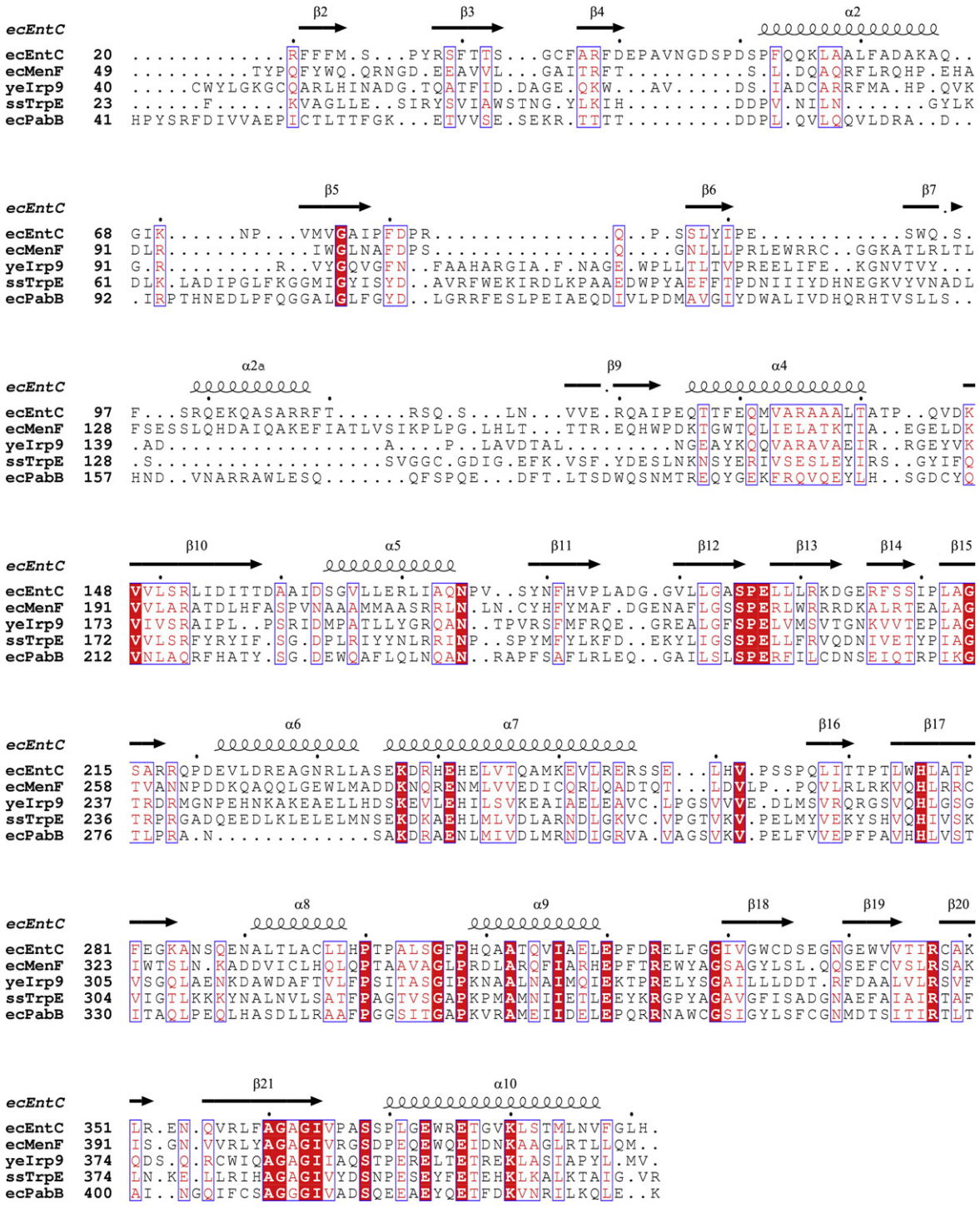

Fig. 3. Structure-based sequence alignment of representative chorismate-utilizing enzymes and EntC sequences generated using the ESPript program.[34] ecEntC, *E. coli* enterobactin-specific isochorismate synthase; ecMenF, *E. coli* menaquinone-specific isochorismate synthase; yeIrp9, *Y. enterocolitica* salicylate synthase; ssTrpE, *S. sulfotoricus* anthranilate synthase TrpE component; ecPabB, *E. coli p*-aminodeoxyisochorismate synthase. The highly variable N-terminal sequence is not shown in the alignment. The numbering scheme used for the secondary structure elements of ecEntC follows that of ssTrpE.[15] α2a is unique for ecEntC, which also lacks α1.

3.1 Å from the C2 hydroxyl oxygen. Mutations in this region therefore would be expected to affect activity. The I346L EntC mutant has a 12-fold lower k_{cat}/K_m (chorismate) than the wild type enzyme and the L304A, F359Q double mutation resulted in an enzyme with no detectable activity. The k_{cat}/K_m (chorismate) for the A303T EntC mutant was found to be 130-fold lower than that for wild type EntC. Further, all double, triple and quadruple amino acid substitutions made involving this A303T mutation resulted in an enzyme with no detectable activity. The analogous mutation in MenF (A344T) has been

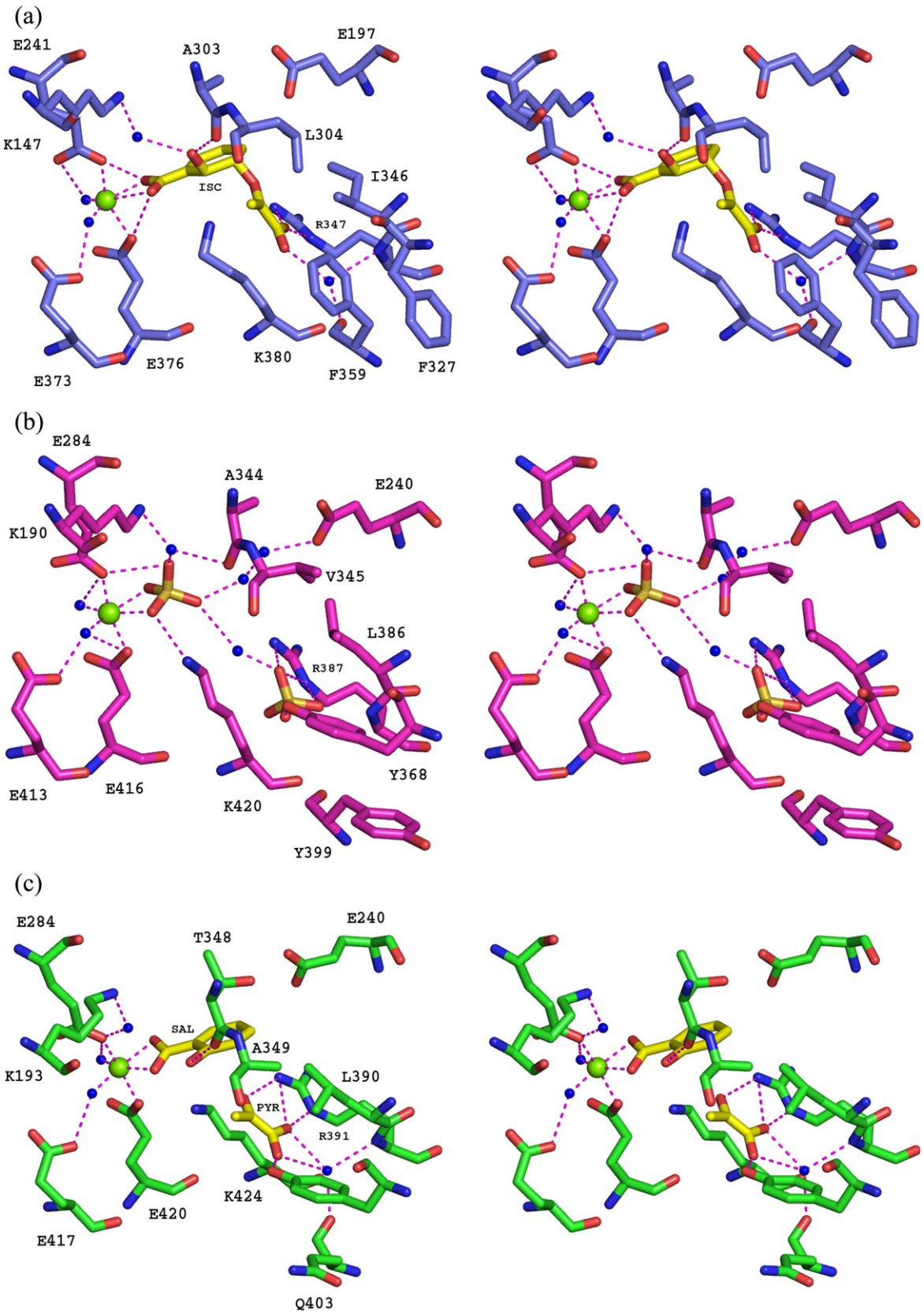

Fig. 4. Active sites of EntC (a), MenF (b) and Irp9 (c). The expected magnesium ion is shown as a green sphere and water molecules are shown as blue spheres. ISC, isochorismate; SAL, salicylate; PYR, pyruvate. For clarity, only some of the hydrogen bonding interactions are shown (dotted lines).

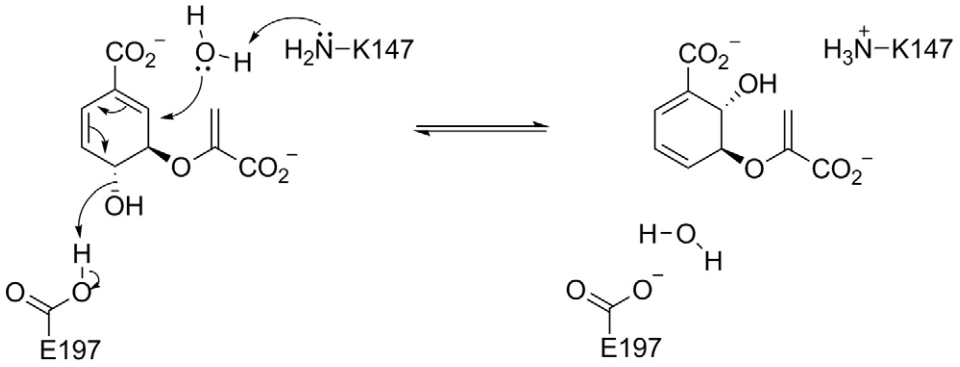

Scheme 1. Proposed mechanism of EntC reaction.

reported to result in complete loss of activity and consequently a role was proposed for this residue in the isomerisation step.[10] For nucleophilic attack at the C2 position of chorismate to give the product with the correct geometry, the water molecule needs to approach the chorismate from the *si*-face, The EntC structure shows that there is an interaction between the backbone carbonyl group of A303 and isochorismate, which suggests a similar interaction between the backbone carbonyl and the water involved in the nucleophilic attack at C4 of chorismate. Changing the size of the side chain of this residue presumably results in some reorientation of the backbone carbonyl, which could well perturb the transition state. The other residue contributing to the *si*-face of water at the C2 position is K147, the lysine being required to activate the water for nucleophilic attack.

The decrease in the activity of EntC incorporating L304A and I346L substitutions shows that subtle changes in the active site affect the ability of the enzyme to hold the substrate in an appropriate conformation for the reaction to proceed. The crystal structure of EntC with the product bound shows that it binds isochorismate in a *pseudo*-axial conformation, which is calculated to be 8.0 – 10.1 kcal/mol less stable than the lowest energy *pseudo*-equatorial conformation.[25] It is postulated that the [3,3] sigmatropic rearrangements from chorismate to prephenate and isochorismate to isoprephenate[26] and the [1,5] sigmatropic re-arrangement from isochorismate to salicylate and pyruvate (Scheme 2) requires adoption of the higher energy diaxial conformation. The active site cavity in EntC is slightly larger than that in Irp9, and possesses a small hydrophobic pocket formed by residues Leu304 and Gly361, which is absent from Irp9. The enol-pyruvyl group binds towards this pocket in such a way that the resultant dihedral angle for C2-C3-O-C8 is 72° with the side chain held away from the central ring. This conformation is unlikely to facilitate the sigmatropic re-arrangements, and could explain both the lack of pyruvate lyase activity of EntC ([1,5] sigmatropic rearrangement) and the absence of side-products associated with [3,3] sigmatropic rearrangements of either substrate (chorismate) and product (isochorismate) observation.[3]

Table 2. Isochorismate synthase activity assay for wild-type and mutant EntC

Mutation	k_{cat} (min^{-1})	K_m (chorismate) (μM)	k_{cat}/K_m (chorismate) (min^{-1} μM^{-1})
Wild type EntC	37	7 ± 0.8	5.3
A303T	4	103 ± 17	0.04
F327Y	8	76 ± 13	0.1
I346L	33	76 ± 8	0.4
F359Q	36	66 ± 10	0.5
F359Q,I346L	11	261 ± 62	0.04
F327Y,I346L	3	466 ± 85	0.006
F327Y,F359Q	26	40 ± 9	0.65
A303T,F327Y	na	—	—
A303T,F359Q	na	—	—
L304A,F359Q	na	—	—
A303T,F327Y, F359Q	na	—	—
A303T,F327Y,I346L	na	—	—
F327Y,F359Q,I346L	na	—	—
A303T,F327Y,F359Q,I346L	na	—	—

na, no detectable activity under experimental conditions.

The differences in orientation of the side chains of F327 and F359 in EntC compared with other chorismate-utilizing enzymes (Fig. 4) prompted investigation of the effects of amino acid substitutions in this region. The F327Y and F359Q mutations resulted respectively in 48-fold and 10-fold lower k_{cat}/K_m than the wild type EntC enzyme. Surprisingly, the F327Y/F359Q double mutation showed only an eightfold reduction in k_{cat}/K_m. It is not clear whether the substitution at position 359 can partially rescue the loss of activity resulting from substitution at position 327. Enzymes with double mutations F327Y/I346L or F359Q/I346L have 750-fold and 130-fold lower k_{cat}/K_m than the wild type enzyme. Comparison of the architectures of EntC, MenF and Irp9 in this region shows that it may be possible for these residues in EntC to be positioned in orientations similar to that in MenF. However, the EntC structure shows that tyrosine at position 327 can be accommodated in the same orientation as the phenylalanine in the wild type enzyme. It has not been possible to reconcile the results of activity assays with structural information as the enzymes incorporating the F327Y and F359Q substitutions could not be crystallised. Studies on the Irp9 Y327F mutant (corresponding to

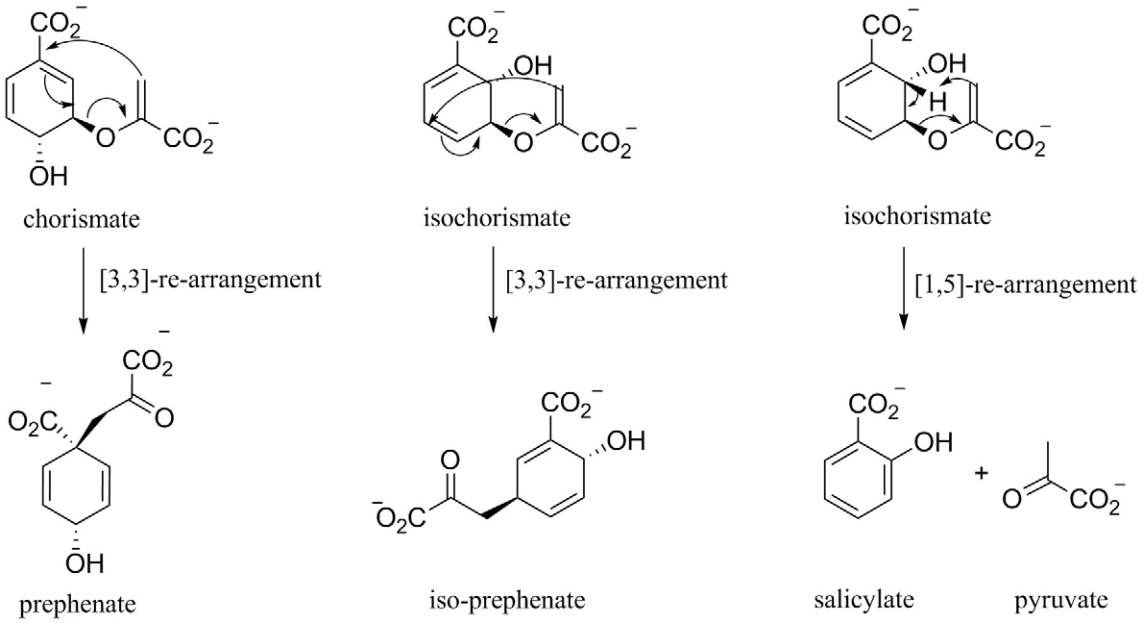

Scheme 2. Sigmatropic re-arrangements of chorismate and isochorismate.

F327 in EntC) confirmed that the tyrosine is not involved in a protonation mechanism for pyruvate elimination in this enzyme.[18]

EntC and related chorismate-utilizing enzymes are involved in essential biosynthetic pathways in pathogenic bacteria. In this context, the availability of the structure of EntC with product bound is important for providing insight into the enzyme mechanism and for the rational design of small molecule inhibitors. Our studies show that although the chorismate-utilizing enzymes all have highly similar active site architectures, subtle differences in the active site residues are enough for these enzymes to acquire a distinct biochemical activity. However, mutagenesis studies have proved to be too blunt a tool to provide a clear picture of precisely how the catalytic activities are differentiated.

Materials and Methods

Cloning, over-expression and purification of EntC

The *entC* gene (1176 bp) from *E. coli* K12 was cloned using the upstream primer: 5′-**CATATG**GATACGT-CACTGGCT-3′ with an *Nde*I restriction site (bold letters) and the downstream primer: 5′-**CTCGAG**TCATTAATG-CAATCC-3′ with an *Xho*I restriction site (bold letters). The amplified product was then digested with the restriction enzymes and ligated with similarly cut pET-28a plasmid DNA (Novagen). The identity of the construct was verified by nucleotide sequencing. For over-expression of EntC, C41 (DE3) or BL21 (DE3) cells (Stratagene) were transformed with the above plasmid containing the *entC* gene. Transformants were selected by growth at 37 °C on Luria-Bertani (LB) agar medium containing kanamycin (50 μg/ml). A single colony was picked and used to inoculate 100 ml of 2×YT medium containing kanamycin (50 μg/ml). This starter culture was used to inoculate 4 l of 2×YT medium. After this culture reached an A_{600nm} of 0.6–0.8 unit, it was cooled to 22 °C. IPTG was added to a final concentration of 1 mM to induce EntC over-expression in the cells and the medium was incubated for 12–14 h at the same temperature with shaking at 220 rpm.

The cells were harvested by centrifugation at 3000 g for 30 min at 4 °C and the pelleted cells were resuspended in buffer A (20 mM Tris pH 7.5, 0.5 M NaCl, 2 mM β-mercaptoethanol) at 4 °C. DNase I at a final concentration of 10 μg/ml and Protease Inhibitor Cocktail (Calbiochem) were added to the suspension before cell lysis using sonication at 4 °C. The crude lysate was clarified by centrifugation at 10,000***g*** for 60 min maintaining the temperature at 4 °C. The clarified lysate was filtered (0.22 μm pore size) before subsequent chromatographic purification steps at 4 °C.

EntC was purified to near-homogeneity using nickel affinity and gel-filtration chromatography, with performance being monitored by SDS–PAGE. The clarified lysate was passed through the Ni^{2+}-charged HiTrap chelating agarose columns (GE Life Sciences) equilibrated with buffer A. The columns were washed with five column volumes of buffer A to remove contaminant proteins. EntC bound to the matrix in the columns was eluted using increasing concentrations of imidazole using buffer B (20 mM Tris pH 7.5, 0.5 M NaCl, 0.5 mM imidazole). The bound protein was found to elute at 150 mM and higher concentrations of imidazole. The eluted protein was concentrated and the buffer changed to buffer C (20 mM Tris pH 7.5, 5 mM magnesium chloride, 1 mM DTT) using a PD-10 desalting column packed with Sephadex G-25 resin (GE Life Sciences). The protein was concentrated and further purified using a XK-16/60 Superdex 75 size-exclusion column (GE Life Sciences) after equilibration with buffer C. The hexahistidine tag of the purified protein was cleaved using thrombin (Novagen) in an overnight reaction performed at 4 °C in a total volume of 50 ml. The sample was concentrated and the size-exclusion chromatographic step described above was done again to remove thrombin and the cleaved hexahistidine tag from EntC. The clones for the various EntC mutant proteins were generated

using the QuikChange site-directed mutagenesis protocol (Stratagene). These mutants were over-expressed and purified using the protocol used for wild type protein as described above. The selenomethionyl derivative of EntC was over-expressed in BL21(DE3) cells using metabolic inhibition procedure.[27]

Enzymatic assays

Salicylate formation by wild type and mutant EntC enzymes was monitored by measuring fluorescence (excitation at 300 nm, excitation at 420 nm). The reactions contained 200–500 nM of wild type or mutant EntC in 100 mM phosphate pH 7.0, 10 mM $MgCl_2$. Isochorismate synthase activity of wild type or mutant EntC enzymes was measured using a coupled enzyme assay with *Pseudomonas aeruginosa* isochorismate pyruvate lyase (PchB) as the second enzyme, which converts isochorismate to salicylate, and monitoring the fluorescence of the salicylate.[28] The assays contained 50 nM wild type or 200–300 nM mutant EntC and 1–3 μM PchB in 100 mM phosphate pH 7.0, 10 mM $MgCl_2$.

Crystallization and data collection

Initial screening for crystallization of EntC was done with 96-well Crystalquick plates (Greiner) and the Cartesian Robot System. Preformatted crystallization conditions, obtained from Qiagen (Classics, Classic Lite and SM1 suite), were screened by mixing EntC protein at concentration of 20–25 mg/ml with an equal volume of the conditions. One of these conditions (100 mM Mes pH 6.5, 12% PEG 20,000) produced crystals in two to three days. Further trials to optimize the conditions to produce bigger crystals were done by the hanging-drop, vapour-diffusion method. Crystals of approximately 0.8–1.0 mm × 0.1 mm × 0.1 mm were produced by mixing one volume of EntC (20–25 mg/ml) and three to four volumes of the above crystallization condition. These crystals were used to collect the X-ray diffraction data. Crystals of the selenomethionyl derivative of EntC protein were produced in the same way as the wild type protein.

X-ray data collection and structure determination

X-ray intensity data were collected at the beamlines PX-10.1 at the Synchrotron Radiation Source, Daresbury, UK (selenomethionyl derivative datasets) and ID-29 at the European Synchrotron Radiation Facility, Grenoble, France (native datasets) under cryogenic conditions. The data collection statistics are given in Table 1. All diffraction data were indexed using Denzo and scaled using Scalepack.[29] Heavy-atom detection and the single isomorphous replacement with anomalous scattering procedure to find phases were done with AutoSharp.[30] We decided to use single isomorphous replacement with anomalous scattering to solve the structure instead of single-wavelength anomalous diffraction, as the former method gave better electron density maps in our study. Protein structural models were constructed using Coot,[31] and CCP4 REFMAC5[32] and the Phenix suite[33] were used for structure refinement.

Protein Data Bank accession number

Coordinates and structure factors have been deposited in the Protein Data Bank with accession number 3HWO.

Acknowledgements

We thank Dr Dima Chirgadze at the Department of Biochemistry, University of Cambridge for help with X-ray data collection and discussion of the EntC structure. We thank the BBRSC for support of this project (RG43711).

Supplementary Data

Supplementary data associated with this article can be found, in the online version, at doi:10.1016/j.jmb.2010.01.019

References

1. Harris, W. R., Carrano, C. J., Cooper, S. R., Sofen, S. R., Avdeef, A. E., McArdle, J. V. & Raymond, K. N. (1979). Coordination chemistry of microbial iron transport compounds. 19. Stability constants and electrochemical behavior of ferric enterobactin and model complexes. *J. Am. Chem. Soc.* **101**, 6097–6104.
2. Ozenberger, B. A., Brickman, T. J. & McIntosh, M. A. (1989). Nucleotide sequence of Escherichia coli isochorismate synthetase gene entC and evolutionary relationship of isochorismate synthetase and other chorismate-utilizing enzymes. *J. Bacteriol.* **171**, 775–783.
3. Liu, J., Quinn, N., Berchtold, G. A. & Walsh, C. T. (1990). Overexpression, purification, and characterization of isochorismate synthase (EntC), the first enzyme involved in the biosynthesis of enterobactin from chorismate. *Biochemistry* **29**, 1417–1425.
4. Rusnak, F., Liu, J., Quinn, N., Berchtold, G. A. & Walsh, C. T. (1990). Subcloning of the enterobactin biosynthetic gene entB: expression, purification, characterization, and substrate specificity of isochorismatase. *Biochemistry* **29**, 1425–1435.
5. Gehring, A. M., Bradley, K. A. & Walsh, C. T. (1997). Enterobactin biosynthesis in Escherichia coli: isochorismate lyase (EntB) is a bifunctional enzyme that is phosphopantetheinylated by EntD and then acylated by EntE using ATP and 2,3-dihydroxybenzoate. *Biochemistry* **36**, 8495–84503.
6. Sakaitani, M., Rusnak, F., Quinn, N. R., Tu, C., Frigo, T. B., Berchtold, G. A. & Walsh, C. T. (1990). Mechanistic studies on trans-2,3-dihydro-2,3-dihydroxybenzoate dehydrogenase (Ent A) in the biosynthesis of the iron chelator enterobactin. *Biochemistry* **29**, 6789–6798.
7. Reichert, J., Sakaitani, M. & Walsh, C. T. (1992). Characterization of EntF as a serine-activating enzyme. *Protein Sci* **1**, 549–556.
8. Nahlik, M. S., Fleming, T. P. & McIntosh, M. A. (1987). Cluster of genes controlling synthesis and activation of 2,3-dihydroxybenzoic acid in production of enterobactin in Escherichia coli. *J. Bacteriol.* **169**, 4163–4170.
9. Nahlik, M. S., Brickman, T. J., Ozenberger, B. A. & McIntosh, M. A. (1989). Nucleotide sequence and transcriptional organization of the Escherichia coli enterobactin biosynthesis cistrons entB and entA. *J. Bacteriol.* **171**, 784–790.
10. Kolappan, S., Zwahlen, J., Zhou, R., Truglio, J. J., Tonge, P. J. & Kisker, C. (2007). Lysine 190 is the catalytic base in MenF, the menaquinone-specific

isochorismate synthase from Escherichia coli: implications for an enzyme family. *Biochemistry* **46**, 946–953.
11. Kwon, O., Hudspeth, M. E. & Meganathan, R. (1996). Anaerobic biosynthesis of enterobactin Escherichia coli: regulation of entC gene expression and evidence against its involvement in menaquinone (vitamin K2) biosynthesis. *J. Bacteriol.* **178**, 3252–3259.
12. Daruwala, R., Bhattacharyya, D. K., Kwon, O. & Meganathan, R. (1997). Menaquinone (vitamin K2) biosynthesis: overexpression, purification, and characterization of a new isochorismate synthase from Escherichia coli. *J. Bacteriol.* **179**, 3133–3138.
13. Dahm, C., Muller, R., Schulte, G., Schmidt, K. & Leistner, E. (1998). The role of isochorismate hydroxymutase genes entC and menF in enterobactin and menaquinone biosynthesis in Escherichia coli. *Biochim. Biophys. Acta* **1425**, 377–386.
14. Buss, K., Muller, R., Dahm, C., Gaitatzis, N., Skrzypczak-Pietraszek, E., Lohmann, S. *et al.* (2001). Clustering of isochorismate synthase genes menF and entC and channeling of isochorismate in Escherichia coli. *Biochim. Biophys. Acta* **1522**, 151–157.
15. Knochel, T., Ivens, A., Hester, G., Gonzalez, A., Bauerle, R., Wilmanns, M. *et al.* (1999). The crystal structure of anthranilate synthase from Sulfolobus solfataricus: functional implications. *Proc. Natl Acad. Sci. USA* **96**, 9479–9484.
16. Morollo, A. A. & Eck, M. J. (2001). Structure of the cooperative allosteric anthranilate synthase from Salmonella typhimurium. *Nat. Struct. Biol.* **8**, 243–247.
17. Spraggon, G., Kim, C., Nguyen-Huu, X., Yee, M. C., Yanofsky, C. & Mills, S. E. (2001). The structures of anthranilate synthase of Serratia marcescens crystallized in the presence of (i) its substrates, chorismate and glutamine, and a product, glutamate, and (ii) its end-product inhibitor, L-tryptophan. *Proc. Natl Acad. Sci. USA* **98**, 6021–6026.
18. Kerbarh, O., Chirgadze, D. Y., Blundell, T. L. & Abell, C. (2006). Crystal structures of Yersinia enterocolitica salicylate synthase and its complex with the reaction products salicylate and pyruvate. *J. Mol. Biol.* **357**, 524–534.
19. Harrison, A. J., Yu, M., Gardenborg, T., Middleditch, M., Ramsay, R. J., Baker, E. N. & Lott, J. S. (2006). The structure of MbtI from Mycobacterium tuberculosis, the first enzyme in the biosynthesis of the siderophore mycobactin, reveals it to be a salicylate synthase. *J. Bacteriol.* **188**, 6081–6091.
20. Parsons, J. F., Shi, K. M. & Ladner, J. E. (2008). Structure of isochorismate synthase in complex with magnesium. *Acta Crystallogr. D* **64**, 607–610.
21. Parsons, J. F., Jensen, P. Y., Pachikara, A. S., Howard, A. J., Eisenstein, E. & Ladner, J. E. (2002). Structure of Escherichia coli aminodeoxychorismate synthase: architectural conservation and diversity in chorismate-utilizing enzymes. *Biochemistry* **41**, 2198–2208.
22. Kerbarh, O., Ciulli, A., Howard, N. I. & Abell, C. (2005). Salicylate biosynthesis: overexpression, purification, and characterization of Irp9, a bifunctional salicylate synthase from Yersinia enterocolitica. *J. Bacteriol.* **187**, 5061–5066.
23. Kerbarh, O., Bulloch, E. M., Payne, R. J., Sahr, T., Rebeille, F. & Abell, C. (2005). Mechanistic and inhibition studies of chorismate-utilizing enzymes. *Biochem. Soc. Trans.* **33**, 763–766.
24. Roux, B. & Walsh, C. T. (1992). p-Aminobenzoate synthesis in Escherichia coli: kinetic and mechanistic characterization of the amidotransferase PabA. *Biochemistry* **31**, 6904–6910.
25. DeClue, M. S., Baldridge, K. K., Kast, P. & Hilvert, D. (2006). Experimental and computational investigation of the uncatalyzed rearrangement and elimination reactions of isochorismate. *J. Am. Chem. Soc.* **128**, 2043–2051.
26. Zamir, L. O., Nikolakakis, A., Bonner, C. A. & Jensen, R. A. (1993). Evidence for enzymatic formation of isoprephenate from isochorismate. *Bioorg. Med. Chem. Lett.* **3**, 1441–1446.
27. Doublie, S. (1997). Preparation of selenomethinyl proteins for phase determination. *Methods Enzymol* **276**, 523–530.
28. Gaille, C., Kast, P. & Haas, D. (2002). Salicylate biosynthesis in Pseudomonas aeruginosa. Purification and characterization of PchB, a novel bifunctional enzyme displaying isochorismate pyruvate-lyase and chorismate mutase activities. *J. Biol. Chem.* **277**, 21768–21775.
29. Otwinowski, Z. & Minor, W. (1997). Processing of X-ray diffraction data collected in oscillation mode. *Methods Enzymol.* **276**, 307–326.
30. Vonrhein, C., Blanc, E., Roversi, P. & Bricogne, G. (2007). Automated structure solution with autoSHARP. *Methods Mol. Biol.* **364**, 215–230.
31. Emsley, P. & Cowtan, K. (2004). Coot: model-building tools for molecular graphics. *Acta Crystallogr. D* **60**, 2126–2132.
32. Dodson, E. J., Winn, M. & Ralph, A. (1997). Collaborative Computational Project 4: providing programs for protein crystallography. *Methods Enzymol.* **277**, 620–633.
33. Adams, P. D., Grosse-Kunstleve, R. W., Hung, L. W., Ioerger, T. R., McCoy, A. J., Moriarty, N. W. *et al.* (2002). PHENIX: building new software for automated crystallographic structure determination. *Acta Crystallogr. D* **58**, 1948–1954.
34. Gouet, P., Courcelle, E., Stuart, D. I. & Metoz, F. (1999). ESPript: analysis of multiple sequence alignments in PostScript. *Bioinformatics* **15**, 305–308.